Nanostructural origin of the spin and orbital contribution to the magnetic moment in $Fe_{3-x}O_4$ magnetite nanoparticles

N. Pérez,[1] F. Bartolomé,[2] L. M. García,[2] J. Bartolomé,[2] M. P. Morales,[3] C. J. Serna,[3] A. Labarta,[1] and X. Batlle[1,a)]
[1]*Dep. de Física Fonamental, Institut de Nanociència i Nanotecnologia (IN2UB), Universitat de Barcelona, 08028 Barcelona, Spain*
[2]*Dpto. Física de la Materia Condensada, ICMA, CSIC-Universidad de Zaragoza, 50009 Zaragoza, Spain*
[3]*ICMM-CSIC, Cantoblanco, 28049 Madrid, Spain*

(Received 2 February 2009; accepted 11 February 2009; published online 5 March 2009)

5 nm $Fe_{3-x}O_4$ nanoparticles were synthesized either by high-temperature decomposition in organic phase or in low-temperature aqueous conditions. In the first case oleic acid was covalently bonded to the nanoparticles; in the second case polyvinyl alcohol (PVA) yielded a protective coating without chemical bond. Magnetization measurements and x-ray magnetic circular dichroism showed a saturation magnetization close to bulk magnetite and an orbital moment effectively quenched in covalently bonded nanoparticles. PVA-coated nanoparticles showed a reduced value of the magnetization and ~3 fold increase in the orbital moment. High resolution electron microscopy suggested that this was related to the nanostructure of the samples. © *2009 American Institute of Physics*. [DOI: 10.1063/1.3095484]

Magnetic nanoparticles (NPs) are an excellent example of nanostructured materials, which have attracted intense research over the recent years, as they provide the critical building blocks for the booming of nanoscience and nanotechnology.[1] They possess an increasing relevance as diagnostic and therapeutic tools in biomedicine.[2] Magnetic NPs for biomedical applications should comply with a variety of requirements including superparamagnetic behavior, large saturation magnetization, limiting size in the order of 20 nm for *in vivo* applications, and biocompatibility and functionality. Iron oxide NPs are relevant for bioapplications due to their low toxicity and ease to be functionalized. Magnetite Fe_3O_4 and maghemite γ-Fe_2O_3 are probably among the most widely studied magnetic materials. However, they still arise much attention. For example, the orbital contribution m_L to the magnetic moment in bulk magnetite is under discussion, where both effective quenching $m_L=0$ (Refs. 3 and 4) and giant m_L (Ref. 5) have been recently reported.

In this letter, we report on the effect of the nanostructure on the magnetic and electronic properties of 5 nm $Fe_{3-x}O_4$ NPs, synthesized either by thermal decomposition of an iron organic precursor in an organic medium[6–9] or coprecipitation of two iron salts in water.[2] In the first case oleic acid was used as surfactant and was covalently bonded to the NP surface due to the high synthesis temperature; in the second case polyvinyl alcohol (PVA) was used due to its excellent adhesive properties, leading to a protective coating against oxidation at the NP surface but without any chemical bond. We show that covalently bonded NPs display bulklike magnetic and electronic properties while NPs with adsorbed coatings show particlelike properties.

Iron oxide $Fe_{3-x}O_4$ NPs were synthesized by two different routes: (i) decomposition at about 250 °C of Fe(III) acetylacetonate in a phenyl ether solution using 1,2-hexadecanediol as reductor and oleic acid and oleylamine as cosurfactants (oleic acid sample)[6–9] and (ii) coprecipitation of $FeCl_2$ and $FeCl_3$ in a NaOH aqueous solution at 50 °C (PVA sample). X-ray diffraction showed very good crystallinity, inverse spinel structure with lattice parameter $a=0.838(2)$ nm, and average crystal diameter 5.8 ± 1.0 nm for the oleic acid-coated NPs and 5.6 ± 1.0 nm for the PVA-protected ones. Low-resolution transmission electron microscopy (TEM) yielded average diameters of 5.2 ± 1.4 and 4 ± 2 nm, respectively (not shown). The oleic acid sample displayed surfactant-coated individual particles with a narrower size distribution, as confirmed by dynamic light scattering (DLS) and energy filtered TEM, while PVA-protected NPs tended to aggregate and showed wider size distributions, as confirmed by DLS. Infrared spectra and thermogravimetric analyses also confirmed the covalent bond in the oleic acid sample.

Figure 1 shows the high-resolution TEM images of both

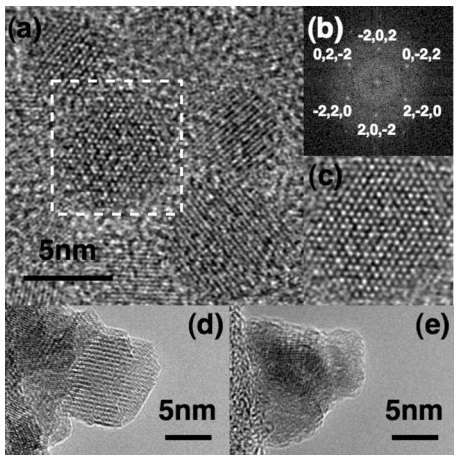

FIG. 1. Oleic acid-coated $Fe_{3-x}O_4$ NPs: (a) high resolution TEM image, (b) Fourier transform of the selected area framed in (a) showing the ⟨111⟩ zone axis, and (c) reconstruction of the direct lattice by inverse Fourier transform using only indexed diffraction spots in (b). PVA-protected $Fe_{3-x}O_4$ NPs: [(d) and (e)] high resolution TEM images. Note that the scale bars in (a) and (c) are the same.

a)Electronic mail: xavierbatlle@ub.edu.

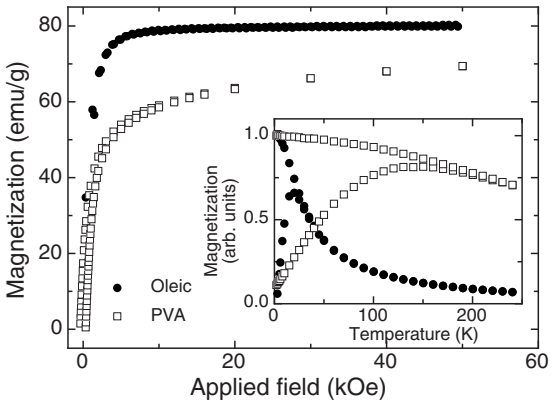

FIG. 2. Magnetization curves $M(H)$ at 5 K for the oleic acid (solid dots) and PVA (empty squares) samples. Inset: ZFC/FC curves measured at 50 Oe for the same samples.

samples. Oleic acid coated NPs show high crystal quality up to the particle surface. The Fourier transform of the selected area in Fig. 1(a) yields the diffraction pattern in Fig. 1(b), which can be indexed to the ⟨111⟩ zone axis of the iron oxide fcc structure. Figure 1(c) shows the reconstruction of the lattice by inverse Fourier transform using only the indexed diffraction spots in Fig. 1(b). In contrast, PVA-coated NPs in Figs. 1(d) and 1(e) show a more irregular shape and a lower degree of crystallinity at the surface together with in-volume defects. This is intrinsic to the coprecipitation method.

Magnetization curves $M(H)$ at 5 K are displayed in Fig. 2. The oleic acid sample saturates at much lower magnetic fields and displays larger magnetization in agreement with the reduction in the surface spin disorder.[10] Saturation magnetization M_s obtained as the extrapolation to zero field from the high-field region in $M(H)$ was found to be $M_s=80.0(1)$ and $M_s=57(1)$ emu/g for the oleic acid and PVA samples, respectively. The former is close to the saturation magnetization of bulk magnetite ($M_s^{\text{bulk}}=98$ emu/g),[11] which is in contrast with the reported values for (coprecipitated) iron oxide NPs ($M_s \approx 50$ emu/g for 4 nm particles[12]), for which the bulk value is not reached up to 100–150 nm.[12] The inset in Fig. 2 shows the zero-field-cooling (ZFC) and field-cooling (FC) magnetizations measured at 50 Oe. For the oleic acid sample, the ZFC evidences a very narrow size distribution through a narrow peak at a temperature $T_{\max}$.[1] The progressive increase in the FC curve below $T_{\max}$ indicates the absence of relevant dipolar interactions. The fact that the ZFC and FC curves join at $T_{\max}$ suggests that not many aggregates are present in agreement with TEM images and DLS. In contrast, the ZFC/FC for the PVA sample reflects a wider size distribution (the ZFC curve is wider and $T_{\max}$ is higher), particle agglomeration (the ZFC/FC curves join above $T_{\max}$), and non-negligible interparticle interactions.

X-ray absorption spectroscopy (XAS) and x-ray magnetic circular dichroism (XMCD) experiments at the $L_{2,3}$ Fe edges were performed at the ID08 beamline of the ESRF in Grenoble at 5 K and in an applied field of 1 T with total electron yield detection and an ~100% polarization rate. In Fig. 3(a), XAS curves are plotted as obtained from the average of the left- and right-circularly polarized light absorptions. Once normalized to the absorption edge jump obtained in a bulk sample well above the edges ($E_N \sim 750$ eV),[13,14]

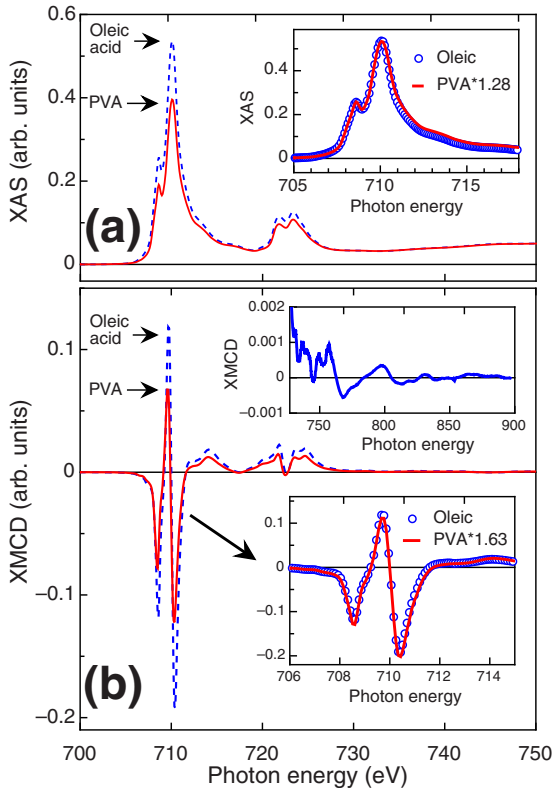

FIG. 3. (Color online) (a) XAS curves at the $L_{2,3}$ Fe edges measured on the oleic acid (dashed blue line) and PVA (solid red line) samples. The inset shows a detail of the scaling of the Fe L_3 edge of both samples. (b) XMCD curves at the $L_{2,3}$ Fe edges recorded on the oleic acid (dashed blue line) and PVA (solid red line) samples. Upper inset: detail of the high-energy XMCD curve of the oleic acid sample. Bottom inset: detail of the scaling of the XMCD curves at the Fe L_3 edge measured on both samples.

the white line for the oleic acid sample is 28% higher than that obtained in the PVA sample, indicating that the number of 3*d* holes in the Fe 3*d* band is considerably enhanced by the charge transfer associated with covalent coating. Quantitative analysis of the XAS data leads to a total number of 3*d* holes $N_h=17.5(3)$ for the oleic acid sample, as compared to $N_h=13.5(2)$ in bulk Fe_3O_4.[13,14] The PVA coating does not affect N_h significantly [$N_h=13.7(3)$]. Figure 3(b) shows the XMCD curves of both samples being their shape similar to that reported by Park *et al.*[6] for a variety of iron oxide NPs. Moreover, the XAS and XMCD curves of the oleic acid and PVA samples are identical once the signal of the PVA sample is multiplied by a factor of 1.28 and 1.63, respectively [see the insets in Figs. 3(a) and 3(b)]. That scaling factor in the XAS data reflects the change in N_h while the one in XMCD also includes the difference in the magnetic moment. The scalability of XAS and XMCD supports that both samples have essentially the same stoichiometry. From the comparison of the XMCD spectra to those for bulk magnetite and maghemite,[6,14] a composition of about $Fe_{2.83}O_4$ is obtained. This result is compatible with the presence of up to 50% of γ-Fe_2O_3 in the form of an overoxidized shell surrounding the particle core. This is in good agreement with Ref. 6 and results from the fact the magnetite and maghemite form a solid solution. Therefore, the 40% increase observed in M_s for the oleic acid sample as compared to the PVA sample [$M_s(\text{PVA})/M_s(\text{oleic})=0.712$], for particles showing the same size and stoichiometry, may be related to a decrease in

TABLE I. Total number of $3d$ holes N_h, magnetic moment per formula unit μ_L (orbital), μ_S (spin), μ_{Fe} (total), and orbital-to-spin moment ratio m_L/m_S for oleic acid and PVA samples.

Sample	N_h	$\mu_L(\mu_B)$	$\mu_S(\mu_B)$	$\mu_{Fe}(\mu_B)$	m_L/m_S (%)
Oleic acid	17.5(3)	0.036(8)	3.24(5)	3.27(6)	1.1(3)
PVA	13.7(3)	0.081(9)	2.25(3)	2.31(3)	3.6(4)

the magnetic disorder induced by the nature of the protecting layer and/or synthesis procedure.

The sum-rule analysis of the XMCD curves allows obtaining the spin and orbital magnetic moments separately[15] (Table I). The total magnetic moment per formula unit μ_{Fe} in the oleic acid sample is about 42% larger than that for the PVA sample $[\mu_{Fe}(PVA)/\mu_{Fe}(oleic)=0.706]$ in excellent agreement with the magnetization result $[M_s(PVA)/M_s(oleic)=0.71]$. Furthermore, μ_{Fe} for the oleic acid sample is just 16% smaller than that reported from previous XMCD measurements on a magnetite single crystal ($3.90\mu_B$/f.u. from Ref. 3, such that $\mu_{Fe}(oleic)/\mu_{Fe}(bulk)=0.838$), also in excellent agreement with the magnetization result $[M_s(oleic)/M_s(bulk)=0.816]$. Besides, the calculated orbital magnetic moments are 0.036(8) and $0.081(9)\mu_B$/f.u. for the oleic acid and PVA samples, respectively.

As already mentioned, Huang *et al.*[5] found a very large unquenched orbital moment in bulk Fe_3O_4. In contrast, Goering *et al.*[3,4] found a zero orbital moment both in their own data as well as after reanalyzing Huang's results and pointed out that it is mandatory to use an extended energy range to estimate the value at which the XMCD oscillations allow obtaining a proper estimate for the orbital moment. We have used a measurement on a magnetite single crystal up to 900 eV,[13] which is about 150 eV above the highest integration limit used in Refs. 4 and 5. This range includes the relevant high-energy oscillations, as shown in the upper inset of Fig. 3(b). We obtain a m_L/m_S ratio of 0.011(3) and 0.036(4) for the oleic acid and PVA samples, respectively (Table I). Although both values are in qualitative agreement with Goering *et al.*,[3,4] the PVA sample shows about a threefold increase with respect to the expected value $m_L/m_S \approx 0.013$ from local-density approximation calculations for bulk magnetite,[14] as usually found in low dimensional systems and NPs.[16] In contrast, the oleic acid sample fully recovers the value for the bulk orbital-to-spin moment.

In conclusion, thermal decomposition at high temperature of an organic Fe precursor allows the preparation of highly crystalline NPs with bulklike magnetic properties, while low-temperature coprecipitation leads to a particlelike system. We have correlated the nanostructure of the NPs arising from the synthesis procedure to their spin and orbital contributions to the magnetic moment. The contribution of the strong electronic bonding and that from the crystal quality cannot be easily decoupled since covalent bond requires high synthesis temperature which in turn leads to good crystallinity. This is a good example of how controlling the nanostructure of materials through the preparation and processing procedures allows to *design* their final properties.

The financial supports of the Spanish MEC (Grant Nos. NAN2004-08805-C04-02, NAN2004-08805-C04-01, MAT2006-03999, MAT2008-01077, MAT2008-01489, and CSD2006-00012), Catalan DURSI (Grant No. 2005SGR00969), and Aragonese DGA (DECRYPT) are recognized. The authors thank A. G. Roca (ICMM-CSIC) for sample preparation, P. Guardia (IN2UB) for TEM, and J. C. Cèzar (ERSF-Grenoble) for making available to us unpublished data and for assistance during experiments.

[1] X. Batlle and A. Labarta, J. Phys. D **35**, R15 (2002).
[2] P. Tartaj, M. P. Morales, S. Veintemillas-Verdaguer, T. González-Carreño, and C. J. Serna, J. Phys. D **36**, R182 (2003).
[3] E. Goering, S. Gold, M. Lafkioti, and G. Schütz, Europhys. Lett. **73**, 97 (2006).
[4] E. Goering, M. Lafkioti, and S. Gold, Phys. Rev. Lett. **96**, 039701 (2006).
[5] D. J. Huang, C. F. Chang, H.-T. Jeng, G. Y. Guo, H.-J. Lin, W. B. Wu, H. C. Ku, A. Fujimori, Y. Takahashi, and C. T. Chen, Phys. Rev. Lett. **93**, 077204 (2004).
[6] J. Park, K. K. An, Y. Hwang, J.-G. Park, H.-J. Noh, J.-Y. Kim, J.-H. Park, N.-M. Hwang, and T. Hyeon, Nature Mater. **3**, 891 (2004).
[7] A. G. Roca, M. P. Morales, K. O'Grady, and C. J. Serna, Nanotechnology **17**, 2783 (2006).
[8] N. Pérez, P. Guardia, A. G. Roca, M. P. Morales, C. J. Serna, O. Iglesias, F. Bartolomé, L. M. García, X. Batlle, and A. Labarta, Nanotechnology **19**, 475704 (2008).
[9] P. Guardia, B. Batlle-Brugal, A. G. Roca, O. Iglesias, M. P. Morales, C. J. Serna, A. Labarta, and X. Batlle, J. Magn. Magn. Mater. **316**, e756 (2007).
[10] X. Batlle, X. Obradors, M. Medarde, J. Rodríguez-Carvajal, M. Pernet, and M. Vallet-Regí, J. Magn. Magn. Mater. **124**, 228 (1993).
[11] B. D. Cullity, *Introduction to Magnetic Materials* (Addison-Wesley, Reading, MA, 1972).
[12] G. F. Goya, T. S. Berquó, and F. C. Fonseca, J. Appl. Phys. **94**, 3520 (2003).
[13] J. C. Cèzar (private communication).
[14] H.-T. Jeng and G. Y. Guo, Phys. Rev. B **65**, 094429 (2002).
[15] B. T. Thole, P. Carra, F. Sette, and G. van der Laan, Phys. Rev. Lett. **68**, 1943 (1992).
[16] F. Luis, F. Bartolomé, F. Petroff, J. Bartolomé, L. M. García, C. Deranlot, H. Jaffrès, M. J. Martínez, P. Bencok, F. Wilhelm, A. Rogalev, and N. B. Brookes, Europhys. Lett. **76**, 142 (2006).